World Journal of Advanced Research and Reviews
eISSN: 2581-9615 CODEN (USA): WJARAI
Cross Ref DOI: 10.30574/wjarr
Journal homepage: https://wjarr.com/

(RESEARCH ARTICLE)

Check for updates

Microstructural, physico-mechanical and thermal characterization of materials based on epoxy resin reinforced of palm kernel shell powder Tenera type for a view to a structural application

Frédéric Djoda Pagoré [1, 2, *], Saïdjo [3], Valentin Makomra [4], Alain Danebé Kada [5], Richard Ntenga [3] and Louis-Max Ayina Ohandja [4]

[1] *Laboratory of Mechanics and Production Engineering (LMPE), Doctoral Training Unit in Engineering Science, University of Douala, P.O. Box 27, Douala, Cameroon.*
[2] *Civil Engineering and Architecture laboratory of the National Advanced School of Engineering, University of Maroua, P.O. Box 46 Maroua Cameroon.*
[3] *Laboratory of Analysis, Simulations and Tests (LAST), University Institute of Technology, University of Ngaoundéré, Cameroon.*
[4] *Laboratory of Materials Mechanics, Structures and Integrated Manufacturing, National Advanced School of Engineering, University of Yaoundé 1, P.O. Box 8390 Yaoundé, Cameroon.*
[5] *Laboratory of Textile and Leather Engineering of the National Advanced School of Engineering, University of Maroua, P.O. Box 46 Maroua Cameroon.*

World Journal of Advanced Research and Reviews, 2025, 25(03), 1471-1485

Publication history: Received on 08 February 2025; revised on 16 March 2025; accepted on 19 March 2025

Article DOI: https://doi.org/10.30574/wjarr.2025.25.3.0853

Abstract

This work promotes the use of palm kernel shell powders associated with epoxy resin for the design of composite materials. Powders identification is carried out by FTIR analyses with vibrational movements. The crystalline character highlighted by DRX. The processing conditions with temperature favored the good behavior of the samples obtained with epoxy resin. A good behavior in water is observed on these samples. The best density result is the formulation T08_05_0125 which gives 1.9799 kg/m^3, 1.8052 kg/m^3 for T08 and 1.7719 kg/m^3 for T05 and T0125. These results follow those of the compressive strength where the composition T08_0.5_0.125 gives the best results, namely 39.59KN for the 20/80 formulation, 37.17KN at 30/70, 36.92KN at 40/60 and 36.25KN at 10/90. These results follow those of the compressive strength where the composition T08_0.5_0.125 gives the best results, namely 39.59KN for the 20/80 formulation, 37.17KN at 30/70, 36.92KN at 40/60 and 36.25KN at 10/90. These results are those improved by to the temperature influence on the constituents during implementation. The compressive strengths in these particular temperature conditions are improved by 24.46% on average compared to those achieved at room temperature. The thermal behavior of the particles studied by TDA/TGA analysis made it possible to specify their capacity to contain heat and that for which the powder retains its intrinsic properties. These materials can be used in structural elements of mechanical engineering and civil engineering.

Keywords: PKS-Powders; Microstructure; DTA/TGA; RE; Physical Properties; Mechanical Behavior

1. Introduction

Composite materials have seen great success in engineering in recent years with innovative and less expensive resources. The environmental impacts limitation due to the excessive use of fossil resources [1,2] has directed researchers towards sectors offering alternative solutions in vegetation. Thus, materials from plant resources are increasingly encouraged [3 – 5]. Composites based on thermoplastic and/or thermosetting polymers [6,7] are

* Corresponding author: Frederic Djoda Pagoré

increasingly combined with renewable resources [8] due to their biocompatibility [9,10] and biodegradability [11]. Waste from agro-industry, often thrown into nature, is rehabilitated by giving it a new life in innovative structural applications such as the automobile industry and cabinetmaking. Plant fibers are used in the production of lightweight concretes incorporated with expanded clay and flax fibers to evaluate the impact of these components on the physico-mechanical characteristics of concrete and for the reinforcement of mortars [12]. Apart from fibers, surveys are carried out on the shells of palm nuts. In civil engineering, the evaluation of reclaimed asphalt pavement stabilized by the ashes of said shells are used in flexible pavements [13,14]. In mechanical engineering, the formulation of brake pads from these shells (PKS) reinforced with cow bones has also been studied [15]. Likewise, their behavior in polyethylene-co-acrylic acid is studied [16]. The behavior in water and the morphology of these shells have shown that their increase in load has an impact on the material obtained [17]. Composites based on packaging plastics also reinforced with PKS-Fer have seen good use in car bumpers [18]. PKS have also been characterized for their application in water treatment industries. The results reveal that PKS contain morphology and crystalline qualities required as construction and adsorption materials. Their characterization in the sustainable diversification of waste was carried out [19]. Epoxy resin impregnated with plant fibers has been the subject of several studies [20 – 23]. However, these shells rendered into powders have a particularity that we would like to explore from the control of their particle size in the present work. Investigations carried out on these shells do not provide their state of crystallinity on the microstructural scale. A feasibility study of PKS as a replacement for aggregates in lightweight concrete in terms of compressive strength, absorption and density was studied [24 – 27]. The exploration of new materials reinforced with wood species, such as olive wood combined with polypropylene [28,29] or other biodegradable bio composites [30] has interested researchers. But the microstructure of these new types of raw materials remains very little known. Failure to control the behavior of these powders in composites does not offer a perfect application in engineering [31,32]. Certainly, polypropylenes associated with particulate reinforcements in panels have mechanical properties [33] that could be improved. Epoxy matrix composites reinforced with chopped bamboo and coconut powders were fabricated to evaluate the mechanical behavior. Some work has focused on plant powders in the form of nanoparticles in studies on physical properties such as bulk density and compressibility index. Similarly, the physico-mechanical properties of coconut shell particle reinforced composites were fabricated using an epoxy matrix. The behavior of the constituents at interphase and interfacial cohesion has never been elucidated although epoxy resin has proven itself in the composites processing conditions under temperature [34 – 36]. In the present work, the palm nut shells are crushed and their particle size is controlled. A microstructural characterization will be carried out to highlight the intrinsic values from a molecular, morphological and thermal bonding point of view. It will also be question of proposing an exact formulation depending on the particles size to optimize the mechanical properties and their use.

2. Material and methods

2.1. PKS_T Presentation

The reinforcements used are waste from Tenera model palm nut shells (PKS_T) obtained following the refining process, then rendered into powders. This organic matter is essentially composed of organic cells and fibrovascular bundles.

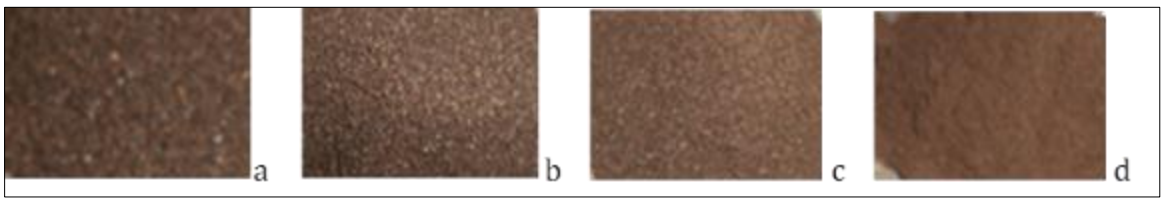

Figure 1 Surface morphology of PKS_T Powder (a)T_{08}, (b)T_{05}, (c)T_{0125}, (d)T_{004}

These powders are obtained using a high-end vibro sieve consisting of a column of superimposed analytical sieves (STS J-4 Digital High Frequency Sieve Shaker). Particle size ranges from 40 to 800 µm. (Figure 1).

2.2. Chemical and thermal treatment of PKS_T powders.

These hulls have previously undergone a chemical treatment using NaOH soda, then dried for several days in the sun before being crushed. The treatment induces the alteration of the structures of the cellulose powders and then the different chemicals can be used on the surface of the powders in order to improve the interfacial properties. The shells were pretreated with 8% NaOH for 2 hours of immersion and stirring in water at room temperature in order to rid them of fat and subsequently to activate the –OH groups of the cellulose and lignin in the powder.

2.3. Fourier Transform Infrared (FT-IR) Spectroscopy

The chemicals bonds and clay materials surface functional groups were determined by FT-IR. The experiment was performed on a Bruker Alpha-P spectrometer (Thermo Electron) in absorbance mode. The spectra were recorded within the spectral range (400 - 4000) cm^{-1} with a resolution of 4 cm^{-1}.

2.4. Structure Analysis by X-Ray Diffraction (XRD)

In order to ascertain the structural information of the studied sample powders, XRD analysis was carried out using a diffractometer from Bruker (Cu anticathode Kα1 (λ = 1.5406 Å, λ = 1, 5418 Å, V = 40 kV, I = 30 mA). The analysis was performed over 2° < 2θ < 70° (Step size: 0.02° and time per step 2s), in the Bragg-Brentano θ/θ configuration. Peak intensities of XRD patterns used for both qualitative and semi-quantitative was approximate [37].

2.5. Thermal analysis of PKS_T

Thermal experiment was investigated on palm kernel shell to bring out the transition signals correlated phase changes. The analysis was performed on a SetaramLABevo TG-DSC 1600°C dispositive, running under Argon flow. Starting from the room temperature, samples were heated up to 1200°C within a ramp of 10 to 40°C·min-1. The TDA/TGA survey were run in an air flow, with Al2O3 crucibles.

2.6. Scanning Electron Microscopy (SEM)

The morphology at the microscopic scale was analysed on a Philips microscope model XL30 with high-voltage accelerated electron beams. The CM samples were regularly disposed on a sample supporter and then installed in a SEM yard maintained in a vacuum of 5 × 10 cm-2 Pa.

2.7. Resin used

In this study, SR 8200/SD 7203 epoxy resins are used as structural adhesives. These thermosetting resins have enjoyed great success in the field of fibrous composites with vegetable fillers. They offer a very wide choice of responsiveness for the production of large series parts. It has the advantage of having low toxicity, good mechanical performance and affordable cost. The SD 7302 hardener is chosen because of its good mechanical properties at room temperature. It distinguishes itself from other resins by its high mechanical characteristics, without shrinkage, colorless, odorless and completely non-toxic, its thermal resistance, its resistance to chemicals and hydrocarbons. Resistance to UV and aging are better. Epoxy resin is also a good insulator, recommended for coating electrical components.

2.8. Composites manufacturing

Several series of mixtures have been established in various formulations. The implementation in this study uses the mixture pouring technique. The epoxy resin is mixed with the PKS_T powders at different particle sizes until homogenized before polymerization for 24 hours in the mold. The compression molding device is used to promote internal bonds and accelerate the crosslinking process of the constituents. A 10T hydraulic press is used to carry out compaction and ensure good dispersion of the powders in the matrix while respecting the conditions imposed by the resin manufacturers. In addition, everything was taken up again by bringing the resulting mixture to a temperature of 250°C. The compressive strength will be given depending on the mixture.

Table 1 Various mixture

Samples		**PKS_T$_{08}$**				**PKS_T $_{05}$**				**PKS_T$_{0125}$**				**PKS_T $_{08\_05\_0125}$**			
Mixture (wt%)	resin	10	20	30	40	10	20	30	40	10	20	30	40	10	20	30	40
	PKS_T	90	80	70	60	90	80	70	60	90	80	70	60	90	80	70	60

Each type of particle is mixed 10/90, i.e. 10% resin and 90% reinforcement up to 40/60. This is for all particle sizes studied.

2.9. Water absorption test

Water absorption studies were carried out on these composites made from epoxy resin reinforced with PKS_T in water at room temperature subjected to bad weather. The initial masses of the prepared samples were recorded. Then they are immersed in bowls containing water. After 24 hours, they are removed from the bowls and wiped dry using a dry

cloth. The operation was repeated every 24 hours for 8 days and the water absorption percentage (Mt) was calculated as follows:

$$Mt = \frac{W_n - W_d}{W_d} \times 100 \qquad \text{.....(1)}$$

Where Wd and Wn are the masses measured before and after quenching, respectively.

2.10. Density of the samples

The mass of each sample is obtained after weighing using the high-precision 30K3L electronic balance. The volume of the samples being known, the density is calculated by the relationship Density = mass of the sample / volume of the sample.

2.11. Strength properties determination

The tests are carried out on the samples obtained using the TVH series 200KN compression and bending testing machine. The results are shown in Figure 9 and 10.

3. Results and discussion

3.1. Physical properties

3.1.1. Water adsorption capacity

The good behavior of certain samples after the water absorption test is partly explained by the adsorption property which characterizes palm nut shells [38]. Indeed, the presence of cellulosic fibers on these shells is responsible for both rigidity and resistance to humidity. Thus, we witness the creation of interfacial forces through the fixation of water molecules and consequently the establishment of mechanical connections between the particles and the matrix. The quantity of powders and the dosage of the resin do not significantly influence the absorption of water in the material. The open porosity linked to the irregular shape of the particle surfaces (T08) can theoretically be filled with water without it penetrating. Preheating the constituents accelerates internal cohesion at the interphase zones, responsible for multiple chemical reactions; which allows the material to acquire the expected properties. Reason why all curves end asymptotically horizontal (figure 2).

The observed absorption kinetics of the granular particles are evaluated. It is reflected on all absorption curves. Samples made from T08 powders absorb water quite quickly during the first 24 hours. It becomes saturated after 3 to 5 days. In this enclosure, a moisture content of 11% on average is achieved for types T08, with 4.5% for T05 and 4% for T0125 (Figure 2).

The compound pattern of T08 powders has a relatively high moisture content due to the high roughness that allows water to remain in the surface cavities of these types of particles, which does not promote good dispersion and distribution of the resin. This creates porous voids responsible for the early penetration of water molecules.

For the specific 10/90 blend, the small amount of resin fails to fill the irregularly shaped cavities left by the grinding operation. This concavity is thus filled by stagnant water; which explains the water saturation. This is not the case when the quantity of resin is at 30% and 40% (Figure 3) for the assembly consisting of T_0.8_0.5_0.125. All these curves tend asymptotically due to the adsorption power possessed by the PKS_T powders.

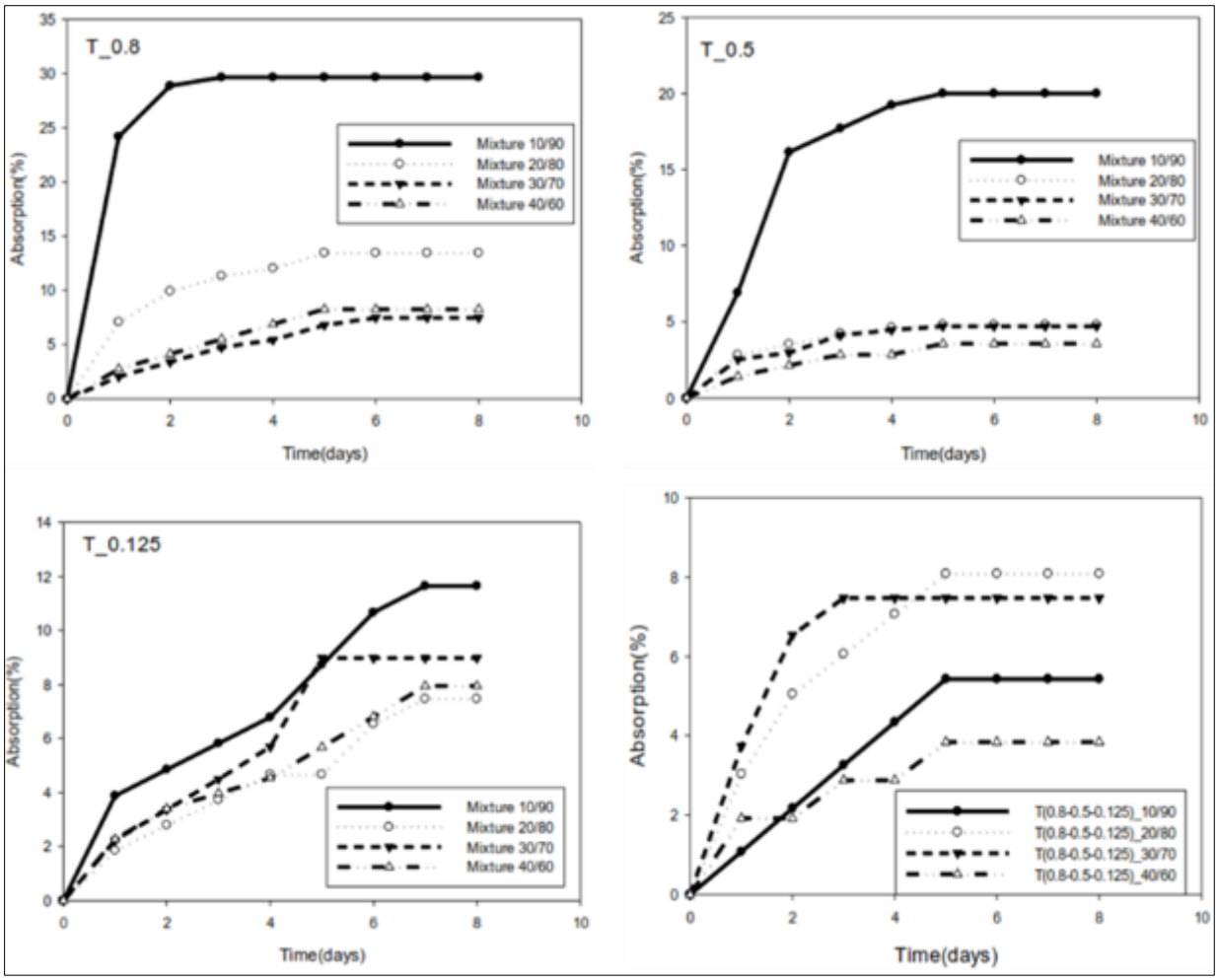

Figure 2 Water absorption of samples

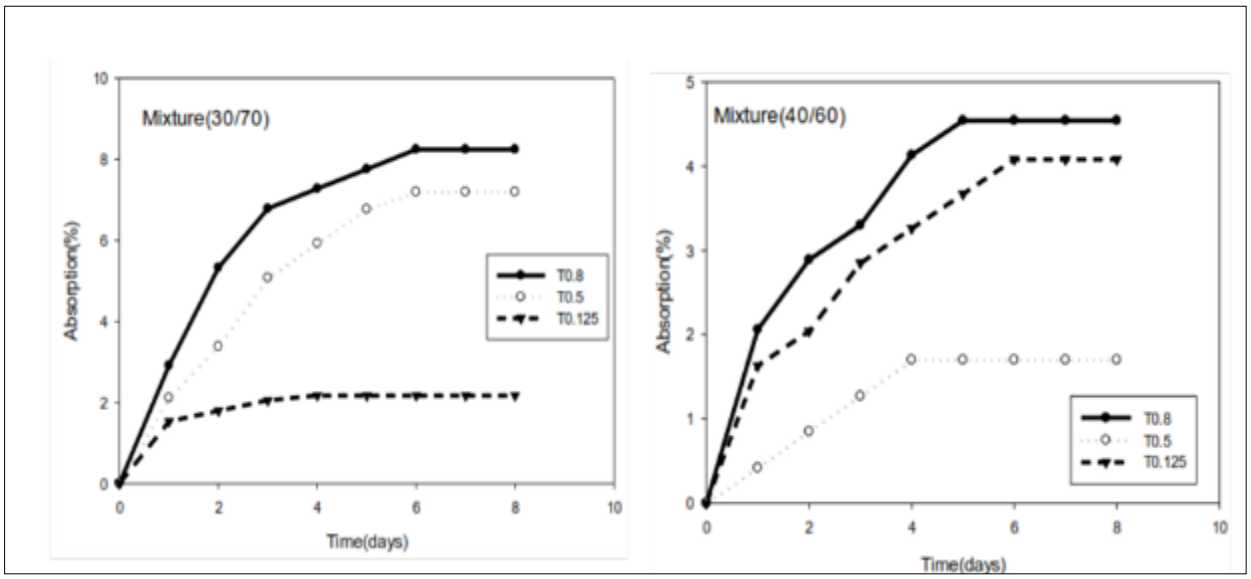

Figure 3 ll formulations at 30/70 and 40/60

3.1.2. Density

Density is one of the most important physical properties of particleboard materials. The obtained density of these materials as a function of the formulation is presented in Figure 4. The decrease in density can be linked to the fact that the PKS_T particles are light and absorb very little water.

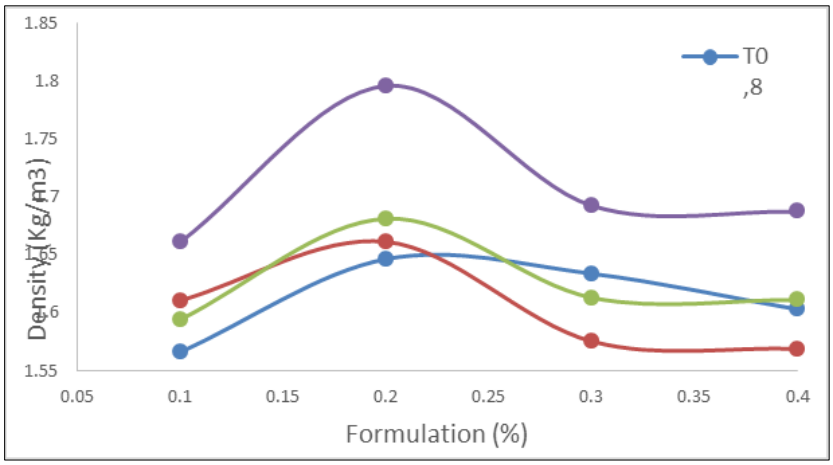

Figure 4 Density according the PKS particles percentage

We observe two behaviors. The density increases with the percentage of resin to reach a maximum of 20%; this for all compositions. The best results are recorded for the formulations of T08_05_0125. This is explained by the rheological capacity of small particles to be able to reorganize themselves and adopt privileged positions. Above 20%, the density begins to decrease up to 40% resin percentage. We are witnessing a reduction in the particles which constitute the charges within the material. Thus, the powders of these test pieces constitute the supporting elements of the composites produced. Their low percentage in favor of resin does not favor their density.

Samples designed with T08 particles show poor results compared to others. This reflects the fact that the very irregular topography of their surface does not favor the rearrangement of particles, infiltration and filling of concave zones during compaction. The low density of the resin used compared to that of the powders is also an explanation.

The good behavior of the T_{0125} particles is explained by their more rounded shapes. The spherical shape of these powders is very suitable for good rearrangement of particles during the compaction operation. This is why the larger the particle size of the powders, the lower the density profile, as this facilitates porosity within the material.

The adsorption properties of these powders open up a real opportunity for retention of the matrix layer in order to create a real interphase zone conducive to the consolidation of composites. Hence the mastery of structural properties to verify the types of molecular bonds in each of the interfaces of the constituents of the materials to be produced.

3.2. Structural and microstructural analyzes

3.2.1. Infrared analysis

The spectra obtained by infrared analysis (IRTF) of samples of Ténéra type palm nut shells treated with soda are illustrated in Figure 5. The vibration bands characteristic of these powders was assigned in accordance with the literature [39, 40] and based on the main spectra obtained. Each peak is illustrative of an attachment to a specific type of bond, responsible for the consolidation of physico-mechanical phenomena within the composites designed from said powders. The presence of OH group is identified with the broad band around 3335 cm-1 of the aromatic and aliphatic structures of phenols of the lignin and cellulose groups. This grouping of adjacent configuration creates unsaturation to give rise to C=C bonds around the peak at 1505 cm-1 [41] followed by an increase in intensity of the band around 1610 cm-1 attributed to the valence vibration of the H-O-H double bond. The bump-shaped band around 2800 cm-1 corresponds to the asymmetric elongation vibration of the C-H bond of cellulose. [42]

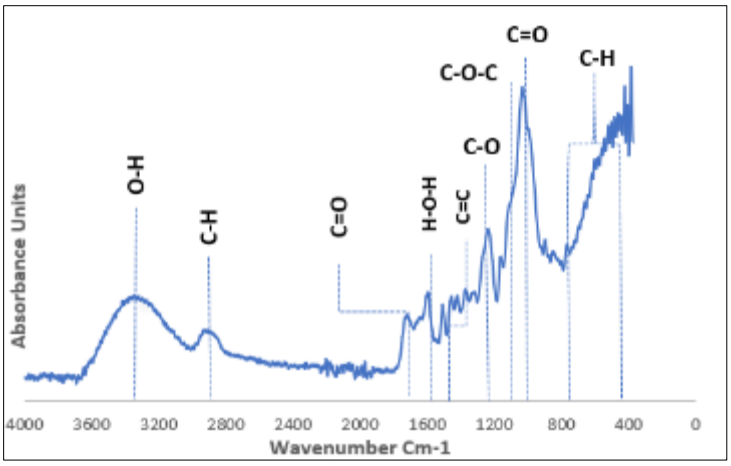

Figure 5 Infrared spectra of Ténéra powder sample

The peak at 1705 cm-1 is characteristic of the valence vibration of the C=O group of carboxylic acids and xylan esters, present in lignins and hemicelluloses [43,44]. Its appearance in the cells of palm nut shells presages their predisposition to establish strong chemical bonds in the constitution of composite materials. The bands observed at 1317 cm-1 correspond to the C-O vibrations of the methoxyl groups in the aromatic structure of celluloses and lignins. The peak at 1025 cm-1 corresponds to the valence vibrations of the C=O and C-O-C bonds of cellulose [45,46]. The peak at 894 cm-1 and the bands which appear at the frequency between 720 - 400 cm-1 are characteristic of the C–H group [47] in the cellulose of plant materials [48,49].

3.2.2. X-ray diffraction (XRD analysis)

The crystallinity of samples of Tenera type palm nut powders obtained at different particle sizes is evaluated in this paragraph by X-ray diffraction (XRD). The results presented in Figure 6 display spectra that are characteristic of the physical and structural properties of plant materials. Thus, the spectra of these four samples display quite diverse main 2Θ peaks. The highest peak is observed at 26.82° and another broad-spectrum peak (hump) from 20 to 23°. Indeed, the zone going from 14.41 to 27.64° with several other peaks dotted around, for example 34.65° and 47.31°, characterize the zones with high crystallinity. [50 – 52] Which indicates the presence of crystalline and semi-crystalline regions in all four samples of these Tenera-type palm nut particles. This predisposes them to good crosslinking during the formation of strong mechanical bonds in the establishment of composite materials. None of these four curves presents a typically amorphous zone; although this state exists. The size of the particles really had no influence on the structural character of the diffractograms in this figure 6 with the presence of the finest particle $T_{0.04}$.

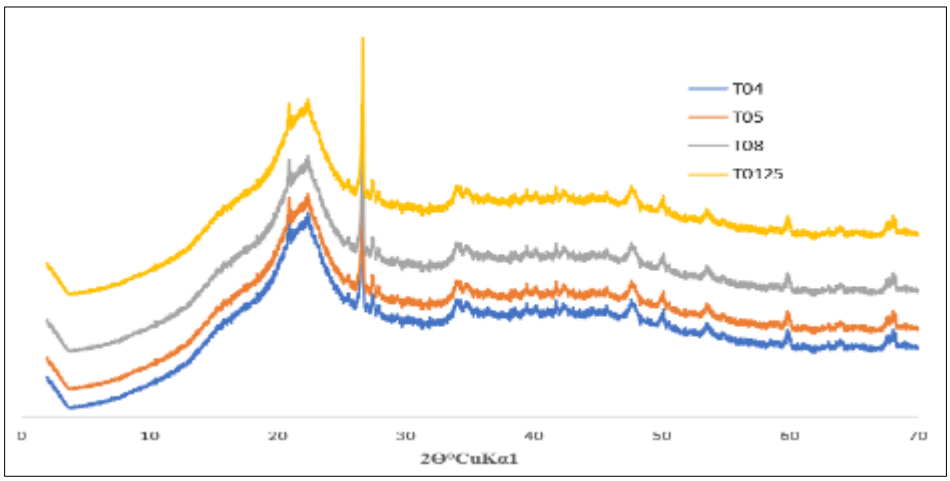

Figure 6 X-ray diffraction patterns of T_{08}_T_{05}_T_{0125}_T_{004} powders samples

This crystallinity will promote the resumption of amorphous zones which are represented by the presence of lignocellulosic fibers and subsequently modify the crystallization kinetics in the same way as the crosslinking phenomenon within the polymers. Which is in harmony with the results of the FTIR analysis.

3.2.3. SEM analysis

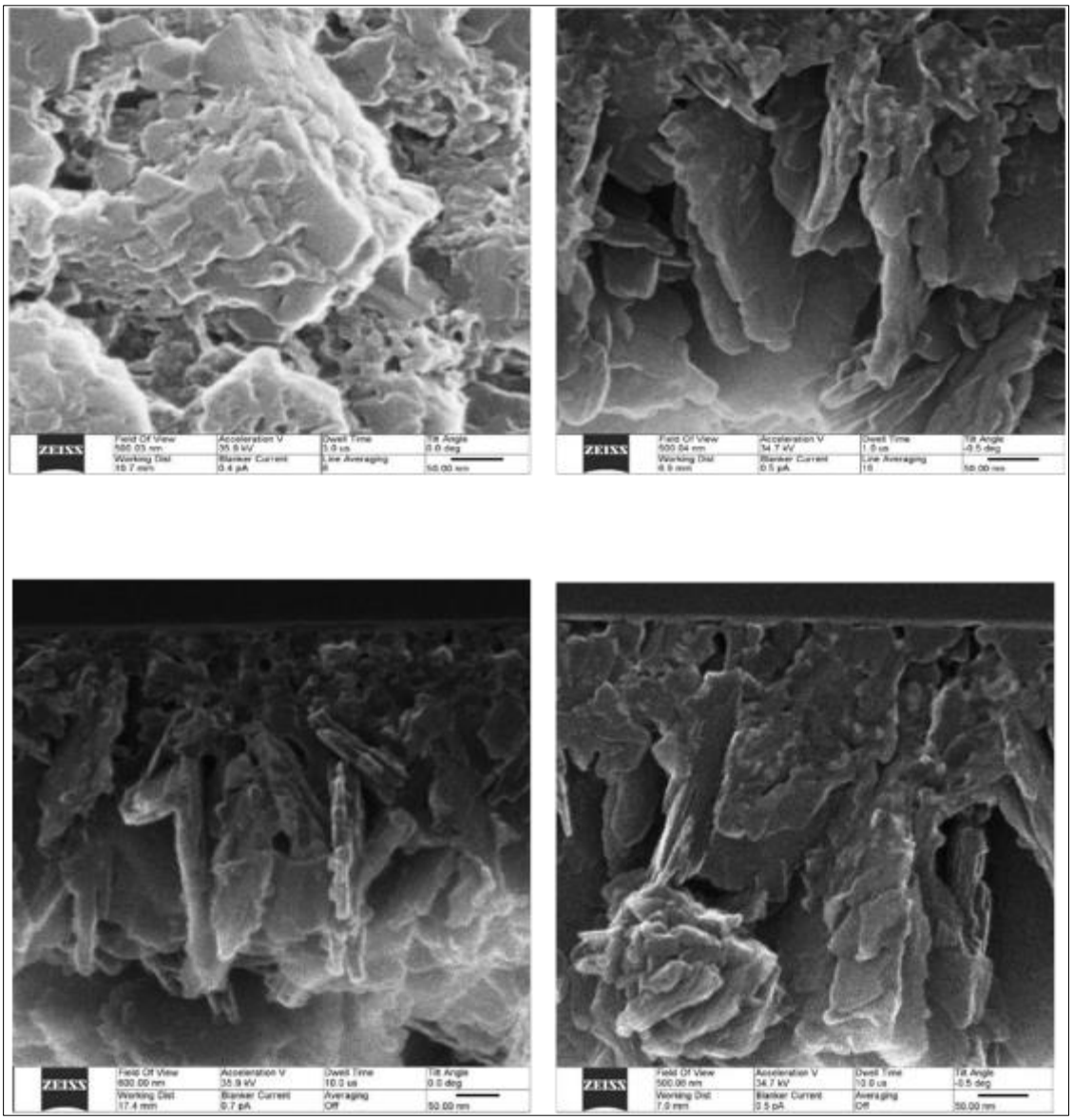

Figure 7 Morphological images of samples from T_{08}_T_{05}_T_{0125}_T_{004} powders

Scanning electron microscopy (SEM) is used in this work to describe the microstructure of the surface of different samples of Ténéra type shells with varied grain sizes after chemical treatment. The different SEM microphotographs of these treated samples (since the IRTF and XRD analysis means showed the effectiveness of the pretreatment) are presented in Figure 7. These images generally reveal a morphology characterized by more or less irregular exterior surfaces and structural heterogeneities observed on either side of these four samples. The fineness of sample T004 with its enlargement to 600nm displays more elongated agglomerations with specific surfaces well materialized on each isolated structural layer. Sample T08 shows the presence of intercellular voids in the form of cavities with varied and predominant circular concavities. This shape is characteristic of its capacity to retain water and fluids of all other kinds.

The illustration of the T0125 particles reveals platelets and superpositions of horizontal tubes which reveal fluid circulation paths. These are known as tracheids which are elongated cells with outlets in the form of furrows ensuring the conduction of the fluid matrix. We also observe obstacles in varied undulations marked and punctuated by differences in height visible on the scale of the SEM images. These zones are the places of exchange of substances with

adjacent cells and promote the adsorption mechanism. The micrograph of sample T05 illustrated here shows a pile of tracheids in a more disordered structure because they have superimposed and tiered arrangements on the one hand, and on the other hand we observe scattered densified agglomerations. This leaves porosity spaces favoring the hydrolysis and flow of lower particles as for T08. The porosity observed in these samples reflects the degradation of hemicelluloses and the elimination of extractable materials following the structural modification of the cellulose. [53]

3.2.4. Analyse thermique

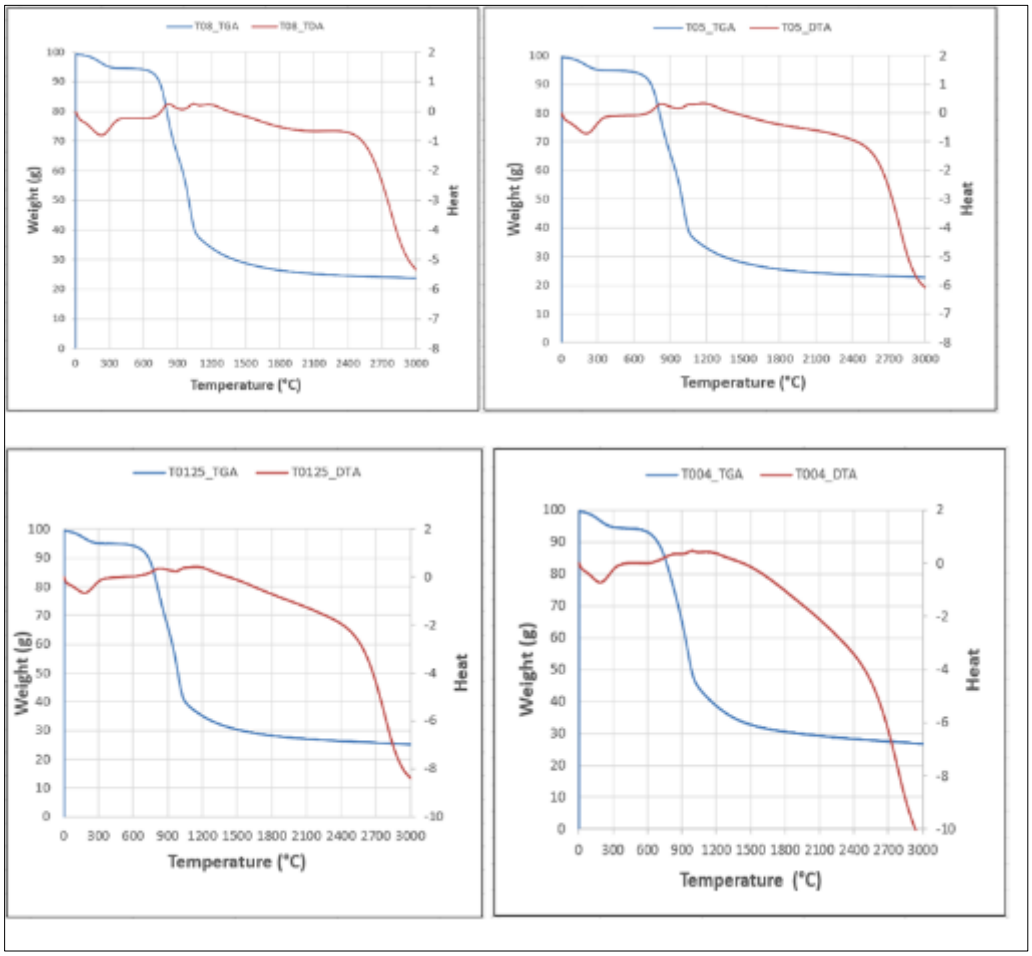

Figure 8 DTG/TGA curves of materials from T_{08}_T_{05}_T_{0125}_$T_{08_05_0125}$ samples

Differential thermal analyzes are carried out to obtain information on the thermal behavior of PKS Tenera powders tested in a temperature range beyond 1200°C.

The start of the transformation process for these four samples begins at just over 100°C. The temperatures vary with the size of the sample powders revealed, namely 149°C for T08, 133°C for T05, 127°C for T0125 and 115°C for T004. Furthermore, the temperatures of 251°C for T08, 221°C for T05, 209°C for T0125 and 206°C for T004 are those which mark the total loss of the slightest trace of humidity and also signify the end of this first phase of transformation. These different temperature peaks characterize the first phases of the mass loss of each of these samples. Sample T08 loses 4.37%, T05 loses 4.53%, T0125 4.81% and T004 4.88%. The second phase shows us that these four samples lose 35% of their mass for a temperature of 900°C. Beyond this temperature, the TGA curve changes concavity and begins the start of decomposition to return to the temperature at which these powders will turn into ashes. On the TGA curve of T08, it is 1075.56°C with a slight exothermic peak of the TDA curve which marks this same process of final decomposition of this powder material. It should be remembered that these powders completely lose their constituents around 971°C on average before being definitively converted into ashes.

The loss of mass by the ATG presented in Figure 8 attests that the Tenera type palm nuts rendered into powders retain all the intrinsic capacities and qualities at a temperature of 671.95 °C for the four samples tested. It is beyond this temperature that the loss of its molecular qualities begins.

The heat flow, directly dependent on the heat capacity of the material and its variation, results in endothermic and exothermic peaks on the thermograms. The curves in Figure 8 show endothermic peaks observed for these four powder samples attributed to the gradual departure of water particles [54]. This stage is followed by a renewed slope which is neither an exothermic nor an endothermic phase but which can be attributed to a form of crystallization accompanied by a progressive degradation of hemicelluloses and cellulose [55] observable on all these curves.

Beyond 671.95°C, all the curves of the four varieties of powders experience a drop in slope up to 1054°C for all particle sizes before starting irreversible decomposition. We witness the thermal decomposition of the lignin contained in all these powders [56].

3.3. Mechanical analysis: Compressive Strength of composites

The poor topography of the $T_{0.8}$ particles does not favor a good equilibrium arrangement at the interphase level. This negatively impacts the phenomenon of interfacial adhesion, responsible for the establishment of ionic bonds to ensure physical and mechanical performance.

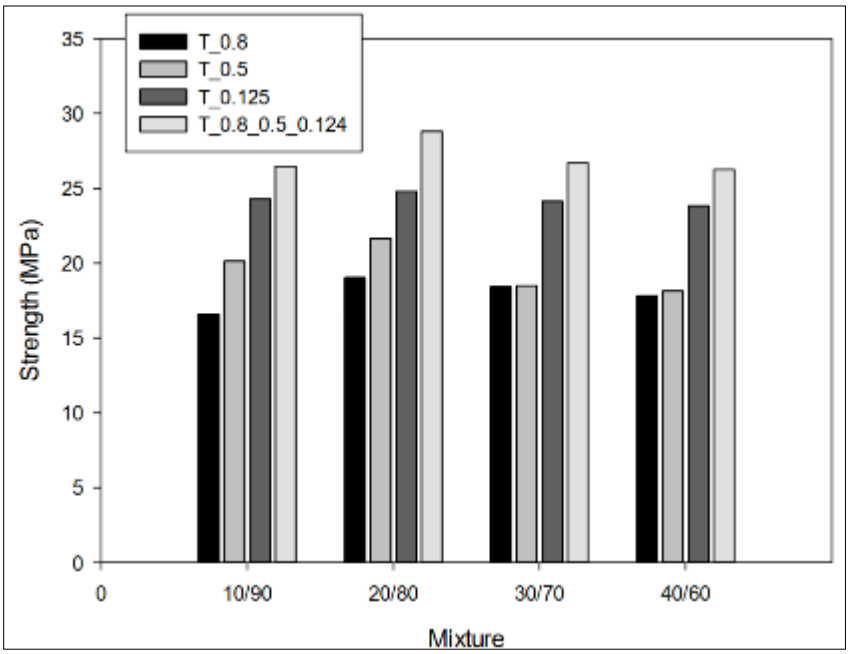

Figure 9 Compressive strength as a function of particles sizes

In terms of resin dosage, the 20/80 compositions present the best results in all series combined. Before this value, the quantity of resin seems insufficient. Beyond this value, the quantity of resin is too large and the rheology of the medium does not favor the juxtaposition of the particles during the compaction operation on the one hand, and on the other hand, the quantity of filler or particles remains insufficient. The 10/90 mix, although showing significant results, still needs to be improved by increasing this mix to 20/80. The 30/70 and 40/60 mixes have almost similar results while degrading with the greatest amount of resin.

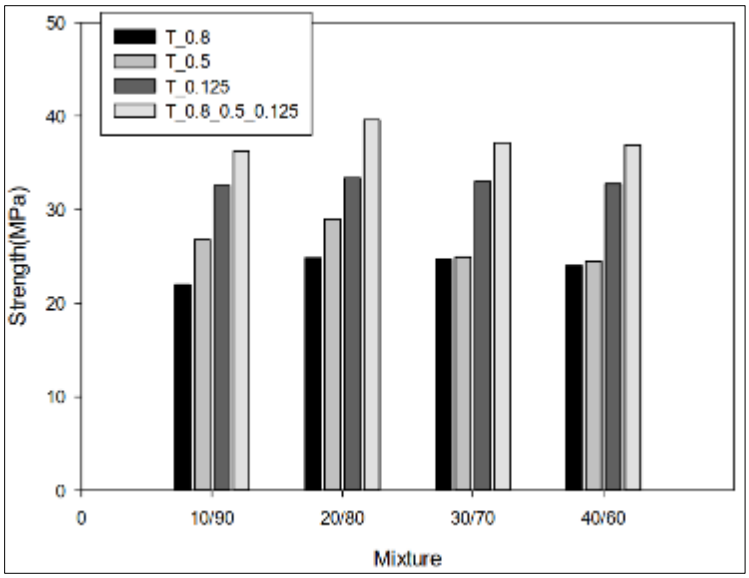

Figure 10 Improvement of compressive strength as a function of particles sizes

Figure 10 shows improved values under the effect of temperature while Figure 9 shows the values obtained under room temperature conditions. The improvement in these values is due to the fact that the temperature favors the rheology of the polymers accompanied by the opening of the functional groups ready to make strong bonds. In addition, the resin becomes more fluid before its polymerization, hence its infiltration and imbibition on all particle surfaces, promoting interfacial bonds between constituents. For these different reasons, the compressive strength values in these particular temperature conditions are up by 24.46% on average compared to the values in Figure 9.

The presence of more materialized specific surfaces on particles of finer sizes demonstrates their ability to receive and retain the matrix where we witness the materialization of strong chemical bonds. This is one of the reasons that show more improved results from materials made from these particles. The other reason is the ease with which finer particles can be well softened and have the ability to adopt privileged positions such as those of the main constraints in the theory of mechanics of continuous media.

3.4. Interpretation of surface chemistry

Chemical analysis of the surface of the palm shell impregnated with a NaOH solution reveals functional groups within the surfaces, favorable to the establishment of atomic bonds originating from the polymer matrix. The specific surface topography and adsorption properties of these powders promote the formation of interfacial interactions and a broad interphase spectrum for polymerization and material consolidation. We will simply say that the interfacial adhesion between powders and matrix finds an environment favorable to crosslinking, hence its success.

4. Conclusion

The investigations carried out on PKS allowed us to have added value on their intrinsic characteristics. Water tests have shown that these powders have remarkable adsorption properties. Indeed, the higher the quantity of resin in the material, the less water the samples absorb. This results on the one hand in the impermeability of the already crosslinked resin. On the other hand, samples with particles of size T08 absorb a little more than the others because their irregular and concave shapes are responsible for the porosity, thus favoring the retention of water particles. In addition, the presence of cellulose fibers promotes the creation of interfacial forces by the fixation of these molecules and therefore the establishment of mechanical connections between particles and matrix. For the 10/90 dosage, the small amount of resin is insufficient to fill the concave shapes on the powder particles left during the grinding operation. Good hold is observed at the 30/70 and 40/60 mixtures, because the resin was able to infiltrate and cover all the irregular shapes on the surface of the powders. The density increases with the percentage of resin up to 20%, then decreases from 20 to 40% for all formulations made under the same experimental conditions. The maximum compressive strength value of 39.59 MPa is that of composition T08_05_0125. This maximum value is greater than that obtained under production conditions at room temperature. We also notice that the smaller the particle size, the higher the density. The best compressive strength results are those from tests on 20/80 formulations. The quantity of resin is just sufficient to ensure good imbibition of the matrix resin over the entire layer of particles. When the shape of the

particle tends to be spherical, the kinetics of the rearrangements of the powder particles due to the rheology of the resin will ensure good distribution of the latter around the different particles. In addition, the series including all particle sizes T0.8_0.5_0.125 shows good results compared to the other series. With a maximum value of 39.59 KN which corresponds to the 20/80 mixture formulation. Indeed, of all the series, the 20/80 mixtures present the best results: 24.85 KN for T08, 28.99 KN for T05, and 33.39 KN for T0125. The quantity of resin for this mixture is necessary and sufficient to ensure good cohesion and good establishment of connections between the constituents put in place. These connections are highlighted by FTIR analyzes carried out on the vibrational movements of the oxides on these powders. They showed the presence of aromatic and planar bonds on the cellulose contained in these plant particles. XRD was able to establish the crystallinity of these PKS for 2Θ angles varying from 18 to 22°C. This favored the crosslinking of chemical bonds and a perfect match between the constituents used, approved by the SEM images. Their thermal behavior favors thermocompression in the production of said materials. Which is the origin of the best loadings of the T0.8_0.5_0.125 series. Gradual compaction explains the fact that small particles with high crystallinity acquire ideal positions to adopt main stresses and directions because of their appropriate morphology. The low values of the T08 series can be explained by their morphological irregularity, a source of porosity within said materials. Thermally, these materials can withstand high temperatures. This predisposes them to structural applications in mechanical engineering as well as in civil engineering.

Compliance with ethical standards

Disclosure of conflict of interest

There is no conflict of interest to be disclosed.

References

[1] Amel Sahki. Development of thermoplastic composites reinforced with basalt and glass fabrics: Study of their durability and recyclability. Materials. IMT - MINES ALES - IMT - Mines Ales School of Mines - Telecom, French. 2022; NNT 2022EMAL0004. Tel-03920064.

[2] Luísa Barroso Gago. In situ creation of a thermosetting phase in a polyolefin matrix by reactive extrusion. Materials. University of Lyon, French. 2021; NNT 2021LYSE1031 tel-03662589.

[3] Chelali, Hamza. Development and physical, mechanical, and dynamic mechanical study of polymer composites based on natural fibers. Doctoral thesis. 2024; Mohamed Khider University (Biskra - Algeria).

[4] P. Dubois, M. Paquot, and H. N. Rabetafika. Plant-derived polymers; materials with specific properties for targeted applications in the plastics industry. Biotechnology. 2006; vol. 10, no. 3, pp. 185–196.

[5] Pierre Bono, Anne Le Duc, Marie Lozachmeur et Arnaud Day. New fields of research and development for the valorization of technical plant fibers (flax fiber and hemp). Materials. 2015; OCL 22(6) D613 https://doi.org/10.1051/ocl/2015041.

[6] Guillaume Gamon. Incorporation of plant fibers into bio-sourced and biodegradable thermoplastic matrices by twin-screw extrusion for the production of injection-molded biocomposite materials. Electrical energy. National Polytechnic Institute of Toulouse – INPT. 2013; NNT: 2013INPT0029, tel-04622453.

[7] F. Constantin. Epoxy-based thermoplastic/thermosetting blends allowing the processing and post-crosslinking of a poly(hydroxy-amino-ether). PhD Thesis. 2003; INSA Lyon.

[8] Franck Gouillou. Dynamic behavior of composites with natural fibers and thermoplastic resins: study of sensitivity to strain rate. Materials. Albi-Carmaux School of Mines. 2024; NNT: 2024EMAC0004. [tel-04818760]

[9] Mohamed RAGOUBI. Contribution to the improvement of the interfacial compatibility of natural fibers/thermoplastic matrix via corona discharge treatment, thesis. 2010; Henri Poincaré University Nancy 1.

[10] CHOUBEILA BOULAARES NASSIMA NOUIOUA. Performance evaluation of two biosupports based on chitosan and functionalized natural alfa fiber for the elimination of an organic pollutant (methylene blue). Doctoral thesis. 2024; Faculty of Science and Technology, University of BBA.

[11] IMENE, CHEBHI. Extraction and Characterization of Microcrystalline Cellulose (MCC) from Date Palm Fibers. Doctoral thesis. 2024; Faculty of Science and Technology, University of BBA.

[12] Zouaoui Abdelkhalek Benbouguerra Taoues. Study of the mechanical, thermal and physical properties of lightweight concrete based on expanded clay reinforced with flax fibers. 2024; https://dspace.univ-bba.dz:443/xmlui/handle/123456789/5399.

[13] J. E. Edeh, J. Manasseh, U. Ibanga. Palm kernel shell ash stabilization of reclaimed asphalt pavements as highway pavement materials. J. Sustain. Dev. Environ. Prot. 2012; vol. 2, nº 1, p. 89–110.

[14] U. G. Eziefula, H. E. Opara, C. U. Anya. Mechanical properties of palm kernel shell concrete in comparison with periwinkle shell concrete. Malays. J. Civ. Eng. 2017; vol. 29, nº 1.

[15] M. Afolabi, O. K. Abubakre, S. A. Lawal, et A. Raji. Experimental investigation of palm kernel shell and cow bone reinforced polymer composites for brake pad production. Int. J. Chem. Mater. Res. 2015; vol. 3, nº 2, p. 27–40.

[16] H. Salmah, A. Romisuhani, et H. Akmal. Properties of low-density polyethylene/palm kernel shell composites: Effect of polyethylene co-acrylic acid. J. Thermoplast. Compos. Mater. 2013; vol. 26, nº 1, p. 3–15.

[17] E. C. Okoroigwe, C. M. Saffron, P. D. Kamdem. Characterization of palm kernel shell for materials reinforcement and water treatment. J. Chem. Eng. Mater. 2014; Sci., vol. 5, nº 1, p. 1–6.

[18] I. A. Samotu, M. Dauda, F. O. Anafi, D. O. Obada, Suitability of Recycled Polyethylene/Palm Kernel Shell-Iron Filings Composite for Automobile Application. Tribol. Ind. 2015; vol. 37, nº 2.

[19] R. S. Fono-Tamo et O. A. Koya, Characterisation of pulverised palm kernel shell for sustainable waste diversification. Int. J. Sci. Eng. Res. 2013; vol. 4, nº 4, p. 43–50.

[20] Anne Hallonet, Laurent Michel, Emmanuel Ferrier. Mechanical behavior of a long flax fiber reinforced epoxy polymer laminated to the contact for the external reinforcement of reinforced concrete structures. Civil Engineering University Meetings. 2015; Bayonne, France. hal-01167600.

[21] Z. Itam, S. Beddu, N. L. M. Kamal, M. A. Alam, et U. I. Ayash, The Feasibility of Palm Kernel Shell as a Replacement for Coarse Aggregate in Lightweight Concrete in IOP Conference Series: Earth and Environmental Science. 2016; vol. 32, p. 012040.

[22] O. P. Oti, K. N. Nwaigwe, et N. A. Okereke. ASSESMENT OF PALM KERNEL SHELL AS A COMPOSITE AGGREGATE IN CONCRETE. Agric. Eng. Int. CIGR J. 2017; vol. 19, nº 2, p. 34–41.

[23] P. Shafigh, M. Z. Jumaat, et H. Mahmud. Oil palm shell as a lightweight aggregate for production high strength lightweight concrete. Constr. Build. Mater. 2011; vol. 25, nº 4, p. 1848–1853.

[24] A. J. Olumuyiwa, T. S. Isaac, O. A. Adewunmi, et A. I. Ololade. Effects of palm kernel shell on the microstructure and mechanical properties of recycled polyethylene/palm kernel shell particulate composites, J. Miner. Mater. Charact. Eng. 2012; vol. 11, nº 08, p. 825.

[25] K.P. JAIN, DR.S.C. SHIT, S.K. JAIN. EVALUATION OF MECHANICAL & THERMAL PROPERTIES OF POLYPROPYLENE – PALM KERNEL NUT SHELL POWDER COMPOSITES FOR GREEN ROOF TECHNOLOGY. 2013; vol. 02, nº ISSUE-02, p. 456-459.

[26] Neslihan Özsoy, Murat Özsoy, Abdullah Mimaroğlu. COMPARISON OF MECHANICAL CHRACTERISTICS OF CHOPPED BAMBOO AND CHOPPED COCONUT SHELL REINFORCED EPOXY MATRIX COMPOSITE MATERIALS. European International Journal of Science and Technology. 2014; Vol. 3 No. 8, p. 15-20.

[27] S. A. Bello, J. O. Agunsoye, J. A. Adebisi, F. O. Kolawole, et B. H. Suleiman. Physical Properties of Coconut Shell Nanoparticles. Kathmandu Univ. J. Sci. Eng. Technol. 2016; vol. 12, nº 1, p. 63–79.

[28] Nesrine Bouhamed. Development and characterization of a composite material based on olive wood flour, PhD thesis. 2020; Normandy University.

[29] Bedreddine Meriem. Study and characterization of new biocomposites of Spanish broom flour-biodegradable polymer, thesis. 2020; FERHAT ABBAS UNIVERSITY - SETIF1.

[30] J. Bhaskar et V. K. Singh. Physical and Mechanical Properties of Coconut Shell Particle Reinforced-Epoxy Composite. J Mater Env. Sci. 2013; vol. 4, nº 2, p. 227–232.

[31] X.-C. Yu, D.-L. Sun, D.-B. Sun, Z.-H. Xu, et X.-S. Li. Basic properties of wood ceramics made from bamboo powder and epoxy resin. Wood Sci. Technol. 2012; vol. 46, nº 1-3, p. 23–31.

[32] S. C. Kavalastrahiremath, B. Siddeswarappa, et T. H. M. Abhishek. A Study on Compressive Strength and Water Absorption Behaviour of Coconut Coir and Coconut Shell Powder Reinforced Natural Composites. International Journal of Research in Advent Technology. 2016; Vol.4, No.5, E-ISSN: 2321-9637.

[33] A. Mahfoudh, A. Cloutier, et D. Rodrigue. Characterization of UHMWPE/wood composites produced via dry-blending and compression molding. Polym. Compos. 2013; vol. 34, nº 4, p. 510–516.

[34] Sofien Bouzouita. Optimization of fiber-matrix interfaces of naturally reinforced composites. Central School of Lyon; National School of Engineering of Monastir. 2011; French. NNT: 2011ECDL0052. Tel-00769959.

[35] Mouatassim Charai. Design and characterization of new bio-sourced eco-materials for sustainable building construction. Thermal [physics. Class-ph]. University of Paris-Est; Mohammed Premier University, Oujda (Morocco). 2021; French. NNT: 2021PESC0068. Tel-03934823.

[36] Quentin Ruiz. Development of bio-sourced epoxy systems for the implementation of dry-impregnated plant fiber composites. Materials. University of Bourgogne Franche-Comté, 2022; French. NNT: 2022UBFCK012. Tel-04140640.

[37] Cook, H.E., Johnson, P.D., Matti, J.C. and Zemmels, I. Methods of Sample Preparation and X-Ray Diffraction. Data Analysis, X-Ray Mineralogy Laboratory, Deep Sea Drilling Project, University of California, Riverside. 1975; Contribution No. 74-5, 999-1007. https://doi.org/10.2973/dsdp.proc.28.app4.1975

[38] H. L. Ong et al. Utilization of Modified Palm Kernel Shell for Biocomposites Production. in Key Engineering Materials, 2016; vol. 700, p. 60–69.

[39] Ouajai S, Shanks RA. Composition, structure and thermal degradation of hemp cellulose after chemical treatments. Polym Degrad Stabil. 2005; 89: 327–335.

[40] M. A. Martín-Lara, F. Pagnanelli, S. Mainelli, M. Calero, and L. Toro. Chemical treatment of olive pomace: Effect on acid-basic properties and metal biosorption capacity. J. Hazard. Mater. 2008; vol. 156, no. 1, pp. 448–457.

[41] Benyoucef et al. Microstructure characterization of scots pine "Pinus sylvestris" sawdust, J. Mater. Environ. Sci. 2015; 6 (3) 765-772.

[42] Manimaran P, Pillai GP, Vignesh V, Prithiviraj M. Characterization of natural cellulosic fibers from Nendran Banana Peduncle plants. International Journal of Biological Macromolecules 2020; 162:1807–15. https://doi.org/10.1016/j.ijbiomac.2020.08.111.

[43] Zheng Zeng, Wentan Ren, Chi Xu Yinxi Zhang. Hydrophobicity Enhancement of Cellulose-Based Material via Heterogeneous Surface Acetylation, Polymers and Polymer Composites. 2009; 17(7) :397-402 DOI: 10.1177/096739110901700701.

[44] T. B. M. Mohd, I. U. H. Bhat, A. L. Mohmod, P. Aditiawati, H. P. S. Abdul Khalil. Thermal and FT-IR Characterization of Gigantochloa levis and Gigantochloa scortechinii Bamboo, a Naturally Occurring Polymeric Composite, Journal of Polymers and the Environment, Springer Science and Business Media LLC. 2012; № 2, p. 534-544 https://doi.org/10.1007/s10924-012-0460-3

[45] Kumar R, Hynes NRJ, Senthamaraikannan P, Saravanakumar S, Sanjay MR. Physicochemical and Thermal Properties of Ceiba pentandra Bark Fiber. Journal of 138 Natural Fibers. 2018; 15:822–9. https://doi.org/10.1080/15440478.2017.1369208.

[46] Karthik T, Murugan R. Characterization and analysis of ligno-cellulosic seed fiber from Pergularia Daemia plant for textile applications. Fibers and Polymers. 2013; 14:465–72. https://doi.org/10.1007/s12221-013-0465-0.

[47] Chen W, Yu H, Liu Y, Chen P, Zhang M, Hai Y. Individualization of cellulose nanofibers from wood using high-intensity ultrasonication combined with chemical pretreatments. Carbohydrate Polymers; 2011; 83:1804–11. https://doi.org/10.1016/j.carbpol.2010.10.040.

[48] Zheng Zeng, Wentan Ren. Hydrophobicity Enhancement of Cellulose-Based Material via Heterogeneous Surface Acetylation. 1958; https://doi.org/10.1177/096739110901700701.

[49] Alemdar A., Sain M. Isolation and characterization of nanofibers from agricultural residues – Wheat straw and soy hulls Bioresource Technology. 2008; Volume 99, Issue 6, Pages 1664-1671 https://doi.org/10.1016/j.biortech.2007.04.029.

[50] Chelali, Hamza. Development and physical, mechanical, and dynamic mechanical study of polymer composites based on natural fibers. Doctoral thesis. 2024; Mohamed Khider University (Biskra - Algeria). http://thesis.univ-biskra.dz/id/eprint/6559.

[51] Chahrazed, G. G. B. Biosynthesis of CuO nanoparticles, characterization and evaluation of their antioxidant activity. Doctoral dissertation. 2023; Faculty of Science and Technology, University of Biskra.

[52] Soundos, R. M. Microcrystalline cellulose from new natural fibers (Isolation and characterization). Doctoral dissertation. 2023; Faculty of Science and Technology, University of Biskra.

[53] H. Kargarzadeh, I. Ahmad, I. Abdullah, A. Dufresne, S. Y. Zainudin et R. M. Sheltami. Effects of hydrolysis conditions on the morphology, crystallinity, and thermal stability of cellulose nanocrystals extracted from kenaf bast fibers. Cellulose. 2012; vol. 19, n° 13, pp. 855-866.

[54] Belaadi A, Bezazi A, Bourchak M, Scarpa F, Zhu C. Thermochemical and statistical mechanical properties of natural sisal fibres. Composites Part B: Engineering. 2014; 67:481–9. https://doi.org/10.1016/J.COMPOSITESB.2014.07.029.

[55] Samanta AK, Basu G, Ghosh P. Structural Features of Glycol and Acrylamide Treated Jute Fiber. 2008; 5:444–60. https://doi.org/10.1080/15440470802453499.

[56] AAyan P, Ashis K S, A Bagchi, Pubalina S, Tapas R K. A Review on Fire Protective Functional Finishing of Natural Fibre Based Textiles: Present Perspective. Curr Trends Fashion Technol Textile Eng. 2020; 7(1): 555705. DOI 10.19080/CTFTTE.2020.07.555705